MOLECULAR AND CELLULAR BIOLOGY, Mar. 2005, p. 2441–2449 Vol. 25, No. 6
0270-7306/05/$08.00+0 doi:10.1128/MCB.25.6.2441–2449.2005

Vascular Endothelial Growth Factor D Is Dispensable for Development of the Lymphatic System

Megan E. Baldwin,[1]† Michael M. Halford,[1]‡ Sally Roufail,[1] Richard A. Williams,[2] Margaret L. Hibbs,[1] Dianne Grail,[1] Hajime Kubo,[3] Steven A. Stacker,[1] and Marc G. Achen[1]*

Ludwig Institute for Cancer Research, Royal Melbourne Hospital, Parkville, Victoria 3050,[1] and Department of Pathology, Faculty of Medicine, Dentistry, and Health Sciences, University of Melbourne, Parkville, Victoria 3052,[2] Australia, and Molecular and Cancer Research Unit, HMRO, Graduate School of Medicine, Kyoto University, Yoshida, Sakyo-ku, Kyoto, Japan[3]

Received 24 August 2004/Returned for modification 10 October 2004/Accepted 7 December 2004

Vascular endothelial growth factor receptor 3 (Vegfr-3) is a tyrosine kinase that is expressed on the lymphatic endothelium and that signals for the growth of the lymphatic vessels (lymphangiogenesis). Vegf-d, a secreted glycoprotein, is one of two known activating ligands for Vegfr-3, the other being Vegf-c. Vegf-d stimulates lymphangiogenesis in tissues and tumors; however, its role in embryonic development was previously unknown. Here we report the generation and analysis of mutant mice deficient for Vegf-d. Vegf-d-deficient mice were healthy and fertile, had normal body mass, and displayed no pathologic changes consistent with a defect in lymphatic function. The lungs, sites of strong *Vegf-d* gene expression during embryogenesis in wild-type mice, were normal in Vegf-d-deficient mice with respect to tissue mass and morphology, except that the abundance of the lymphatics adjacent to bronchioles was slightly reduced. Dye uptake experiments indicated that large lymphatics under the skin were present in normal locations and were functional. Smaller dermal lymphatics were similar in number, location, and function to those in wild-type controls. The lack of a profound lymphatic phenotype in Vegf-d-deficient mice suggests that Vegf-d does not play a major role in lymphatic development or that Vegf-c or another, as-yet-unknown activating Vegfr-3 ligand can compensate for Vegf-d during development.

Vessels of the lymphatic system are highly permeable and specialized for the uptake of fluid and macromolecules from the interstitium and their return to the venous circulation (33). Consequently, the lymphatic vasculature is critical for the maintenance of tissue fluid volume (for a review, see reference 8). It also plays an important role in immune responses, since leukocyte traffic via the lymphatic vessels to lymph nodes is essential for antigen presentation, and in cancer biology, since tumor cells can spread via the lymphatics to establish distant metastases (for reviews, see references 40 and 41). Recent studies with animal models suggested that the growth of the lymphatics (lymphangiogenesis) in and around solid tumors can facilitate the metastatic spread of tumor cells via the lymphatics (21, 29, 39, 42). Lymphedema is another clinical condition in which the lymphatics play a critical role, as inadequate lymphatic drainage of tissue leads to the accumulation of lymph and subsequent swelling of the affected area, a characteristic of this disease (for a review, see reference 8). Elucidation of the molecular mechanisms controlling lymphatic vessel development will underpin approaches to stimulating or inhibiting lymphangiogenesis in clinical contexts, such as lymphedema or cancer, respectively.

Vascular endothelial growth factor receptor 3 (Vegfr-3), a cell surface receptor tyrosine kinase (also known as Flt4), is expressed on lymphatic endothelial cells in adult tissues (18, 27), and its activation is sufficient to stimulate lymphangiogenesis (45). The two known activating ligands for Vegfr-3 are Vegf-c (17) and Vegf-d (also known as c-*fos*-induced growth factor [Figf]) (1, 35), secreted homodimeric glycoproteins that are closely related in structure. In humans, both VEGF-C and VEGF-D activate VEGFR-3 and another receptor, VEGFR-2 (1, 17), which is implicated in signaling for angiogenesis (32); in mice, Vegf-c activates both receptors (23), but Vegf-d activates only Vegfr-3 (6). Thus, the receptor binding specificity of Vegf-d suggests that it may be lymphangiogenic but not angiogenic in the mouse. Indeed, the ectopic expression of VEGF-D in the skin of transgenic mice under the control of the keratin 14 gene promoter induced the growth of lymphatic vessels in the dermis, whereas blood vessels were unaffected (45). In addition, the expression of VEGF-D in a mouse tumor model stimulated lymphangiogenesis in solid tumors; this process promoted the metastatic spread of tumor cells via the lymphatics but could be blocked by a neutralizing VEGF-D antibody (2, 3, 42). The importance of Vegf-c and Vegf-d was further illustrated by the finding that the expression of a soluble form of VEGFR-3 that acts to sequester both growth factors in the skin of transgenic mice caused impaired fetal lymphatic development and a lymphedema-like phenotype (28).

* Corresponding author. Mailing address: Ludwig Institute for Cancer Research, Royal Melbourne Hospital, P.O. Box 2008, Parkville, Victoria 3050, Australia. Phone: (613) 9341-3155. Fax: (613) 9341-3107. E-mail: Marc.achen@ludwig.edu.au.

† Present address: Genentech Inc., South San Francisco, CA 94080-4990.

‡ Present address: Center for Developmental Biology and Kent Waldrep Foundation Center for Basic Research on Nerve Growth and Regeneration, University of Texas Southwestern Medical Center, Dallas, TX 75390-9133.

During early embryonic development, Vegfr-3 is expressed widely on endothelial cells of blood vessels but subsequently becomes restricted to venous endothelium, at a stage prior to the emergence of lymphatic vessels, and then becomes restricted to the endothelium of lymphatic vessels (18, 27). A key role for VEGFR-3 in lymphatic development was demonstrated by the identification of mutations in *VEGFR-3* in several cases of human congenital lymphedema (19). However, mutant mice deficient for Vegfr-3, generated by homologous recombination in embryonic stem (ES) cells, were not informative with respect to lymphatic vessel development or function, as these mice died at embryonic day 9.5 (E9.5) due to defective remodeling and maturation of blood vessels into larger vessels, prior to the emergence of lymphatic vessels from the veins (11). Further studies showed that the Vegfr-3 ligand Vegf-c is required for the initial steps of lymphatic development (20). In *Vegf-c*$^{-/-}$ mice, endothelial cells commit to the lymphatic lineage but do not sprout to form lymphatic vessels. The lack of lymphatic vessels results in prenatal death due to fluid accumulation in tissues. *Vegf-c*$^{+/-}$ mice develop cutaneous lymphatic hypoplasia and lymphedema, demonstrating that both *Vegf-c* alleles are required for normal lymphatic development (20).

To assess the role of Vegf-d in the development of the lymphatic system, we have generated mutant mice that lack Vegf-d by homologous recombination in ES cells. Vegf-d-deficient mice are viable and have a functional lymphatic system. The lymphatic vessels in these mice develop normally and are able to transport fluid to draining lymph nodes. Furthermore, Vegf-d-deficient mice do not display evidence of perturbed lymphatic vessel function. The lack of a profound phenotype associated with Vegf-d deficiency suggests that Vegf-d does not play an important role in lymphatic development or that there is compensation for Vegf-d function during lymphatic development by Vegf-c or another, as-yet-unknown ligand for Vegfr-3.

MATERIALS AND METHODS

Construction of the *Vegf-d* gene-targeting vector. A genomic clone, denoted M18, containing the first and second coding exons of the mouse *Vegf-d* gene was isolated as previously described (7). The short arm of homology (ShA) was derived from M18 and consisted of a 2.5-kb region of the *Vegf-d* gene immediately upstream of the translation initiation codon. ShA was inserted into pZero-2 (Invitrogen) downstream of the cDNA encoding the A fragment of the diphtheria toxin (DTA) gene under the control of the thymidine kinase (TK) gene promoter (the DTA cassette was a gift from S. Tajbakhsh, Departement de Biologie du Developpement, Institut Pasteur, Paris, France). The TK-DTA-ShA DNA then was inserted into the unique BamHI site of pβ-gal-pAlox-neo (a gift from Tracy Willson and Warren Alexander, Walter and Eliza Hall Institute, Melbourne, Victoria, Australia). The resulting plasmid was denoted pDTA-ShA-β-gal-pAlox-neo and consisted of the TK-DTA cassette upstream of ShA, which was in frame with the *LacZ* gene and upstream of the mouse phosphoglycerate kinase gene promoter and the cDNA encoding neomycin phosphotransferase (PGK-*neo*^{r}). The long arm of homology, which consisted of a 6.6-kb EcoRI fragment containing exon 2 and a region of the intron between exons 1 and 2 of the *Vegf-d* gene, was inserted into pSP73 (Promega Corporation) at the EcoRI site to create pSP73-LA. A DNA fragment consisting of TK-DTA-ShA, *LacZ*, and PGK-*neo*^{r} was isolated from pDTA-ShA-β-gal-pAlox-neo by digestion with XhoI and was inserted into pSP73-LA at the SalI site, thereby creating the *Vegf-d* gene-targeting construct, denoted pVDKO-construct.

Generation of Vegf-d-deficient mice. Electroporation of W9.5 wild-type ES cells (2.5×10^7 cells) with 30 μg of pVDKO-construct that had been linearized with XhoI was performed essentially as described previously (9). ES cells were grown on a primary embryonic fibroblast (PEF) feeder layer in the presence of 1,000 U of leukemia inhibitory factor (Chemicon)/ml. Selection with G418 (Invitrogen) at a concentration of 175 μg/ml began 24 h following electroporation and was continued for 9 days, at which time individual colonies were picked and screened for targeting events by Southern hybridization. Genomic DNA from resistant colonies was digested with each of the enzymes HindIII, PvuII, and BglII individually and evaluated by Southern blotting. Blots were hybridized with a 681-nucleotide (nt) fragment of genomic DNA, denoted E1F2R1, that is homologous to a region of the mouse *Vegf-d* gene 5′ to ShA (Fig. 1). E1F2R1 was amplified by PCR with the M18 genomic DNA clone as a template, a sense primer with the sequence 5′-TTTAGTTAGCCCTTTCCTCCA, and an antisense primer with the sequence 5′-TTCTGGGTTGTAGCATAGTCA. Targeted clones were identified at a frequency of 1 of 21, and 2 of them (clones 2.2.36 and 2.88) were injected into C57BL/6J blastocysts and transferred into pseudopregnant mice. Chimeric mice were mated, and the offspring were genotyped by Southern hybridization to identify females carrying a single targeted allele (denoted X^-X^+ because the *Vegf-d* gene is on the X chromosome) and Vegf-d-deficient males (X^-Y). Subsequent mating predominantly involved the breeding of X^+X^+ and X^+Y mice to generate litters consisting entirely of wild-type mice and the breeding of X^-X^- and X^-Y mice to generate litters consisting entirely of Vegf-d-deficient mice. Such offspring were used for experimental phenotypic analyses. Mice designated breeders were the offspring of crosses of wild-type and Vegf-d-deficient mice or were the offspring of crosses of X^+X^- and either X^+Y or X^-Y mice. Breeders were generated in this way to prevent the genetic divergence of wild-type and Vegf-d-deficient mice.

Mice were genotyped by PCR with genomic DNA extracted from the tail tip as a template in a 25-μl PCR mixture consisting of 200 μM deoxynucleoside triphosphates (Amersham Pharmacia Biotech), 2.0 mM $MgCl_2$, 1× AmpliTaq Gold buffer (Applied Biosystems), and 1.25 U of AmpliTaq Gold. The following primers were also added to the PCR mixture: VEGFCM-58 (5′-CTTTCTCCC ATACTAAGATTG; added to a final concentration of 762 nM), which is a forward primer homologous to a region of the *Vegf-d* gene 221 nt upstream of the translation initiation codon; VEGFCM-36 (5′-TCAAACATTCATGGTAAG AAA; added to a final concentration of 1.4 μM), which is a reverse primer homologous to a region 158 nt downstream of exon 1; and GenoRC2Alt (5′-C GCCAGGGTTTTCCCAGTCAC; added to a final concentration of 94.2 nM), which is a reverse primer homologous to a region of the *LacZ* gene 46 nt downstream of the *Vegf-d* translation initiation codon in *Vegf-d* gene-targeted cells (Fig. 1A shows primer positions). The wild-type *Vegf-d* allele was identified with a 461-nt DNA fragment (amplified with primers VEGFCM-58 and VEGFCM-36). The targeted *Vegf-d* allele was identified with a 270-nt DNA fragment (amplified with primers VEGFCM-58 and GenoRC2Alt) (Fig. 1C).

All experiments performed with mice were carried out in accordance with the guidelines set by the National Health and Medical Research Council of Australia.

Derivation of PEF cell lines. PEF cell lines for Northern and Western blot analyses were generated from litters of wild-type and Vegf-d-deficient mice. Embryos were collected at E13.5; the heads and livers were removed, digested with 0.1% trypsin–0.02% EDTA, and sheared by passage through needles of increasing gauge (18, 19, 21, 23, and 25 gauge). Cells were pelleted, resuspended in Dulbecco modified Eagle medium containing 10% fetal calf serum, 2 mM glutamine, and 10^{-6} M β-mercaptoethanol, and transferred to gelatin-coated flasks. Cells were incubated at 37°C in 10% CO_2, and PEFs were passaged 1:2 when a confluent, adherent monolayer had grown. For Northern and Western blot analyses, PEF supernatants and PEFs were collected when the cells were confluent at passage 5.

Northern blot analysis. RNA was extracted from mouse organs and PEF cell lines by the guanidine thiocyanate method essentially as described previously (38). Northern blots were hybridized with a 209-nt PCR product (VDEx7) that had been amplified from *Vegf-d* cDNA by using a sense primer specific to exon 7 (VEGFCM-87: 5′-CTGTGAGGACAGATGTCCTTTTC) and an antisense primer specific to the 3′ untranslated region located in exon 7 (VEGFCM-8: 5′-GGTAGTGGGCAACAGTGACAG). In addition, Northern blots were hybridized with a 425-nt PCR product (VD-VHD) amplified from *Vegf-d* cDNA by using a sense primer specific to exon 3 (VEGFCM-22: 5′-GAAGAATGGCAG AGGACCCA) and an antisense primer specific to exon 5 (VEGFCM-17: 5′-C CAGGCAGTGGAGTCTC). VDEx7 and VD-VHD hybridized to transcripts of the same sizes. Northern blotting for Vegf-c mRNA was carried out essentially as described previously (23).

Western blot analysis. Antiserum A2 (raised against a peptide in the VEGF homology domain [VHD] of human VEGF-D) (43), which binds to the VHD of mouse Vegf-d, or antiserum raised against the DokR protein (26) was incubated with protein A-Sepharose (Amersham Pharmacia Biotech) with rotation for 1 h at 4°C. PEF conditioned medium was added and incubated with rotation for

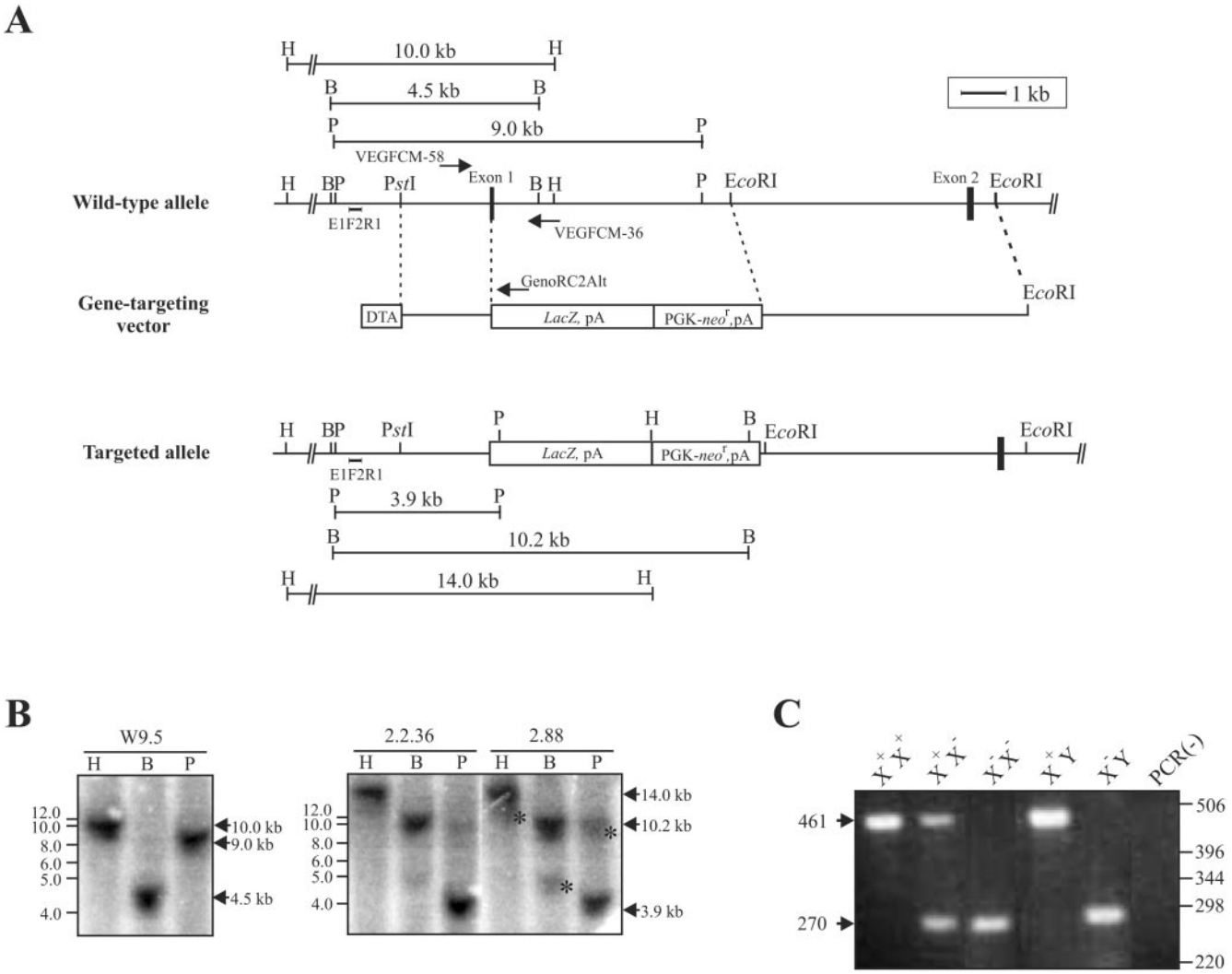

FIG. 1. Generation of Vegf-d-deficient mice. (A) Homologous recombination of the gene-targeting vector at the *Vegf-d* locus (wild-type allele; top) was designed to replace the signal sequence for protein secretion and the remaining sequence of the first coding exon with a *LacZ*-PGK-*neo*^{r} cassette. Construction of the gene-targeting vector (middle) is described in Materials and Methods, and the structure of the targeted *Vegf-d* allele (bottom) is shown. The *Vegf-d* gene consists of seven coding exons (7), but only the first two are shown here. Arrows indicate the positions of primers used to genotype mice by PCR. The position of the PCR-amplified genomic DNA probe, E1F2R1, used to screen ES cell colonies by Southern blotting is shown. The E1F2R1 probe is 5′ to the region of the *Vegf-d* gene that underwent homologous recombination and hybridizes to digested fragments of diagnostic sizes in wild-type and targeted ES cells (the sizes of the relevant fragments are shown at the top and bottom). Restriction sites used to construct the gene-targeting vector or digest genomic DNA for screening are also shown: H, HindIII; B, BglII; P, PvuII. (B) Southern blot analysis of genomic DNA extracted from wild-type (W9.5) and targeted (lines 2.2.36 and 2.88) ES cell clones. Genomic DNA from each ES cell line was digested with HindIII (H), BglII (B), and PvuII (P) and analyzed with the E1F2R1 DNA probe. The asterisks in the 2.88 panel indicate hybridization of the E1F2R1 probe to wild-type DNA fragments derived from copurification of PEF DNA with ES cell DNA. The migration of DNA standards (in kilobases) is shown to the left of each panel. (C) Genotypic analysis of mice by PCR. Primers VEGFCM-58 and VEGFCM-36 amplified a 461-bp DNA fragment from a wild-type *Vegf-d* allele, whereas primers VEGFCM-58 and GenoRC2Alt amplified a 270-bp DNA fragment from a targeted *Vegf-d* allele. Genotypic analysis of wild-type female (X^+X^+) and male (X^+Y), homozygous Vegf-d-deficient female (X^-X^-) and male (X^-Y), and hemizygous female (X^+X^-) *Vegf-d* mice is shown. The migration of DNA size standards (in base pairs) is shown to the right of the panel.

~1.5 h at 4°C. Protein A-Sepharose then was pelleted by centrifugation and washed three times with cold radioimmunoprecipitation buffer (20 mM Tris-HCl [pH 7.5], 150 mM NaCl, 1% Triton X-100, 1% sodium deoxycholate, 0.1% sodium dodecyl sulfate [SDS]). Proteins were eluted by the addition of reducing SDS sample buffer (2% SDS, 10% glycerol, 60 mM Tris-HCl [pH 6.8], 0.02% bromophenol blue, 2% β-mercaptoethanol) and heating to 95°C for 5 min. Proteins were subjected to SDS-polyacrylamide gel electrophoresis (PAGE), transferred to Immobilon P membranes (Millipore), and analyzed by using biotinylated, affinity-purified antiserum (BAF469; 0.2 μg/ml; R&D Systems) raised against amino acids 98 to 206 of mouse Vegf-d (which corresponds to the VHD) and streptavidin-horseradish peroxidase conjugate (Roche Molecular Biochemicals). Development was carried out by chemiluminescence (SuperSignal System; Pierce).

Histological analysis. Excised embryos or mouse tissues were fixed for 3 to 24 h in 4% paraformaldehyde–phosphate-buffered saline, dehydrated, and embedded in paraffin wax. Paraffin sections (5 μm) were stained with hematoxylin and eosin or subjected to immunohistochemical staining with a rat anti-mouse monoclonal antibody to the extracellular domain of mouse Vegfr-3 (22), biotin-conjugated anti-rat immunoglobulin (Dako Corporation), and a tyramide signal amplification (TSA) system according to the manufacturer's instructions (NEN

Life Science Products). As a control, the Vegfr-3 primary antibody was omitted from the procedure. The number of Vegfr-3-positive lymphatic vessels immediately adjacent to the external surface of the muscular layer surrounding bronchioles in age-matched adult lungs was counted by an investigator who was unaware of which sections were derived from wild-type or Vegf-d-deficient mice. The tissue sections used for this analysis were matched for position within the lungs. Three tissue sections were counted per mouse and encompassed at least 130 bronchiole sections per animal.

Measurement of lung fluid volume. Mouse lungs were excised and lightly blotted onto gauze to remove blood acquired during separation from the heart, and the mass was measured (lung wet mass). The lungs then were dried in an oven at 60°C for 3 days, and the mass was measured daily thereafter. The lung dry mass was recorded when the lung mass remained constant over two consecutive measurements. Lung fluid compositions were calculated by subtracting the lung dry mass from the lung wet mass.

Microlymphangiography. Patent Blue 5 dye (Rhone Poulenc Rorer) was injected intradermally into mice anesthetized with xylazine (8 mg/kg)-ketamine (44 mg/kg). The injection site was lightly massaged for 15 min, and the mice were sacrificed by cervical dislocation and dissected to reveal the underlying surface of the ventral skin and the axillary, superficial inguinal, and paraaortic lymph nodes. Uptake of Patent Blue 5 dye into lymphatic vessels was monitored by using a Leica dissecting microscope (model MZ6) and a digital camera. Fluorescence microlymphangiography was performed on mouse tails essentially as described previously (15, 25). Hair was removed from tails 24 h prior to analysis by using depilatory cream. On the day of the experiment, mice were anesthetized with xylazine (8 mg/kg)-ketamine (44 mg/kg). Tetramethylrhodamine-dextran (rhodamine-dextran; molecular weight, 2,000,000; 8 mg/ml; Molecular Probes) was injected subdermally (~50 μl) into the mouse tail tip by using a 30-gauge needle. Mice then were placed on the heated stage (32°C) of a Nikon confocal microscope (model Eclipse TE 300). Uptake of rhodamine-dextran into the superficial lymphatic networks of mouse tails was monitored by confocal microscopy for a period of ~40 min per mouse. The width of the lymphatic vessels and the widest distance between the vessels in each component of the honeycomb lymphatic pattern were measured from the confocal images.

RESULTS

Generation of Vegf-d-deficient mice. As a prelude to the generation of Vegf-d-deficient mice, Southern blot analysis of W9.5 ES cell genomic DNA was carried out with DNA probes homologous to the 5′- and 3′-end regions of the mouse *Vegf-d* gene. This analysis revealed that each probe hybridized to one genomic DNA fragment in each of the digested samples, suggesting that there is only one copy of the *Vegf-d* gene in the mouse genome (data not shown). This finding is consistent with the interspecific backcross analysis, which localized the mouse *Vegf-d* gene to the X chromosome (16). These studies did not reveal any evidence for a second *Vegf-d* gene or a *Vegf-d* pseudogene.

To generate Vegf-d-deficient mice, a gene-targeting vector was used to replace the signal sequence for protein secretion, immediately downstream from the translation initiation site, and the remainder of the first coding exon (Fig. 1A). Correctly targeted ES cells were identified by Southern blot analysis with a DNA probe, E1F2R1, that hybridizes to HindIII, BglII, and PvuII fragments of diagnostic sizes in wild-type and *Vegf-d*-targeted ES cells (Fig. 1B). Eighteen correctly targeted ES cell colonies, out of a total of 384 screened, were identified (targeting frequency, 1 of 21); 2 of these were used to generate independent lines (2.2.36 and 2.88) (Fig. 1B). The 2.2.36 and 2.88 ES cell clones had incorporated a single copy of the *neo*^{r} gene in their genomes, as indicated by Southern blot analysis with a DNA probe homologous to a region of the *neo*^{r} gene (data not shown).

Molecular analysis of Vegf-d-deficient mice. To investigate whether replacement of the first coding exon with a PGK-*neo*^{r} cassette affected the generation of transcripts containing the remaining exons of the *Vegf-d* gene, Northern blot analysis was performed (Fig. 2A). The expression of *Vegf-d* in mice was previously shown to be high in E15.5 embryonic lungs (43). Total RNA was purified from the lungs of wild-type and Vegf-d-deficient E15.5 embryos and subjected to Northern blotting with a probe directed to the 3′ end of the *Vegf-d* gene (VDEx7). The major *Vegf-d* transcripts, of 3.7 and 2.4 kb, in addition to the lower-abundance transcripts, of 3.3 and 2.0 kb, were detected in wild-type E15.5 mouse lungs but not in Vegf-d-deficient E15.5 lungs (Fig. 2A). Because the *Vegf-d* gene is also strongly expressed in PEFs, we confirmed this lack of expression in Vegf-d-deficient mice by generating multiple PEF lines from matings of X^+X^+ and X^+Y mice (wild-type PEFs; this designation is used because the *Vegf-d* gene is on the X chromosome) and matings of X^-X^- and X^-Y mice (Vegf-d-deficient PEFs). In agreement with the Northern analysis of embryonic lungs, a high level of *Vegf-d* expression was detected in all of the wild-type PEF lines, whereas no transcripts of any size could be detected in RNA from Vegf-d-deficient PEFs with this probe (Fig. 2A). Northern blot analysis with a probe homologous to a region of the VHD of Vegf-d (VD-VHD) also detected high levels of Vegf-d expression in wild-type E15.5 lungs and PEF lines but did not detect any transcripts in the RNA derived from Vegf-d-deficient E15.5 lungs or PEF lines (data not shown). These data were also consistent with the results of Northern blot analysis of RNA from mouse line 2.88 and PEFs derived from this line (data not shown).

To further confirm that the targeting strategy resulted in the generation of a null *Vegf-d* allele, conditioned media derived from wild-type and Vegf-d-deficient PEF lines were subjected to immunoprecipitation followed by Western blot analysis with antisera raised against peptides in the VHD of human and mouse Vegf-d (see Materials and Methods). The Western blots demonstrated that the ~21-kDa fully processed subunit of Vegf-d, consisting of the VHD (31, 43), was present in the conditioned medium of wild-type PEFs but not in the conditioned medium of Vegf-d-deficient PEFs (Fig. 2B). In reducing SDS-PAGE, this fully processed derivative consisting of the VHD migrates as two species at ~21 kDa, due to variations in glycosylation. Previous studies indicated that cleavage at the C terminus of the VHD is more rapid than that at the N terminus (43). Consequently, the partially processed derivative consisting of the VHD and the N-terminal propeptide should be relatively abundant compared to the fully processed VHD derivative and other partially processed forms. For human VEGF-D, the size of the polypeptide consisting of the N-terminal propeptide and the VHD is ~31 kDa, consistent with the migration of the N-terminal propeptide at ~10 kDa and of the VHD at ~21 kDa under reducing conditions. This ~31-kDa partially processed form of mouse Vegf-d was abundant in wild-type PEF conditioned medium but could not be detected in that of Vegf-d-deficient PEFs (Fig. 2B). The ~21-kDa mature form and the ~31-kDa partially processed form of Vegf-d were abundant in conditioned media of multiple wild-type PEF lines, whereas Vegf-d could not be detected in conditioned media of any of the Vegf-d-deficient PEFs derived from either of the Vegf-d-deficient mouse lines. The lack of expression of Vegf-d protein in Vegf-d-deficient mutant mice indicates that the gene-targeting strategy created a null *Vegf-d* allele.

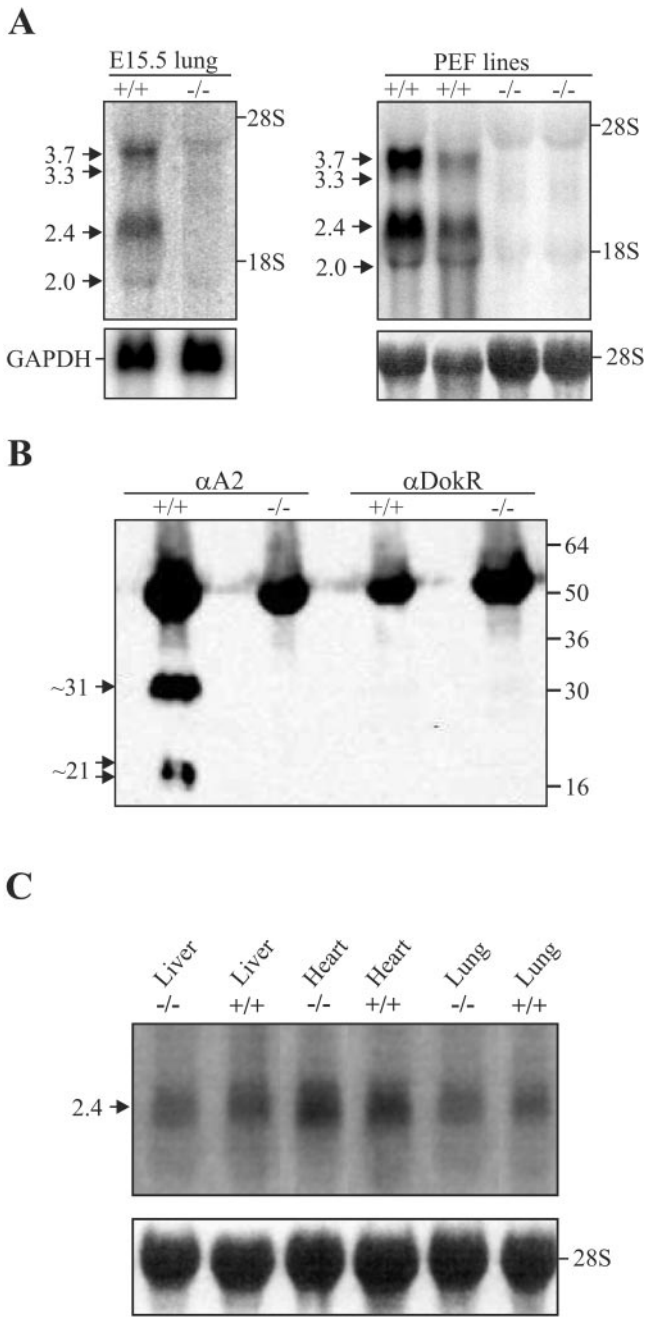

FIG. 2. Northern and Western blot analyses of tissues and cell lines derived from Vegf-d-deficient mice. (A) Analysis of Vegf-d expression in E15.5 lungs (left panel) and PEF conditioned media (right panel) derived from wild-type (+/+) and Vegf-d-deficient (−/−) mice (line 2.2.36). Total RNA was analyzed by Northern blotting with the VDEx7 cDNA probe (the same results were obtained with the VD-VHD probe; data not shown). The signal obtained with a cDNA probe for the glyceraldehyde 3-phosphate dehydrogenase (GAPDH) housekeeping gene is shown as a loading control for E15.5 lung RNA, and methylene blue staining of the 28S rRNA transferred to membranes is indicated as a loading control for PEF RNA. Sizes of *Vegf-d* transcripts (in kilobases) are indicated to the left of the panels. (B) Western blot analysis of conditioned media of PEFs derived from wild-type (+/+) and Vegf-d-deficient (−/−) embryos (line 2.2.36). Conditioned media were incubated with antiserum A2, which binds to the VHD of Vegf-d, or control antiserum raised against the mouse DokR protein (26). The immunoprecipitate was subjected to SDS-PAGE (reducing conditions), transferred to membranes, and blotted with affinity-purified, biotinylated serum raised against the VHD of mouse Vegf-d. The ~21-kDa mature form, consisting of the VHD, and the ~31-kDa derivative, consisting of the N-terminal propeptide and the VHD, were detected in conditioned media of wild-type PEFs but not in media of PEFs from Vegf-d-deficient mice. The specificity of A2 and biotinylated VEGF-D antisera for Vegf-d is indicated by the lack of the ~31- and ~21-kDa proteins when DokR antiserum was used in the immunoprecipitation reaction. The band of ~55 kDa detected in all lanes represents the immunoglobulin heavy chain. The migration of molecular mass markers (in kilodaltons) is shown to the right of the panel. (C) Northern blot analysis of mouse tissues for Vegf-c mRNA. Ten micrograms of total RNA from tissues of adult wild-type (+/+) and Vegf-d-deficient (−/−) mice (line 2.2.36) was hybridized with the Vegf-c probe. The position of the 2.4-kb Vegf-c mRNA is marked to the left of the upper panel, and methylene blue staining of 28S rRNA on the filters is shown in the lower panel as a loading control.

Vegf-d is closely related in primary structure to Vegf-c, and these proteins are both able to induce lymphangiogenesis via the activation of Vegfr-3 (45). It is therefore feasible that the up-regulation of Vegf-c could compensate for Vegf-d function. However, Vegf-d deficiency did not significantly alter the expression of the *Vegf-c* gene, as assessed by Northern blot comparison of Vegf-c mRNA levels in livers, hearts, and lungs from wild-type and Vegf-d-deficient mice (Fig. 2C).

General observations of Vegf-d-deficient mice. Neither female nor male Vegf-d-deficient mice (denoted X^-X^- and X^-Y, respectively) could be distinguished from wild-type mice by morphological appearance. Newborn Vegf-d-deficient mice were observed to suckle and, postweaning, to feed in a manner similar to that of control mice. This finding is reflected in the body masses, which were not different in wild-type and Vegf-d-deficient mice measured at up to 1 year of age (Table 1 shows measurements at 16 weeks). The similar body masses of Vegf-d-deficient and wild-type mice suggest that Vegf-d-deficient mice are able to effectively access, digest, and metabolize food to the same extent as wild-type mice. This suggestion is consistent with observations that Vegf-d-deficient mice displayed levels of activity similar to those of wild-type mice. Vegf-d-deficient mice were fertile, as visibly healthy mice were born from crosses of X^-X^- and X^-Y mice in litters with a mean ± standard deviation number of offspring that was not significantly different (as assessed by the Student *t* test) from that in litters derived from wild-type matings (for wild-type mice, 8.0 ± 2.5 [$n = 26$]; for Vegf-d-deficient mice, 9.3 ± 3.0 [$n = 34$]) ($P = 0.078$). Perturbations in the development and function of the lymphatic system may be reflected in an alteration in interstitial fluid volume leading to swelling of tissue or accumulation of fluid in body cavities. However, there was no visual evidence of altered interstitial fluid volume in the subcutaneous, intraperitoneal, or thoracic regions of Vegf-d-deficient mice, nor was there any accumulation of chyle in the intestines or peritoneal cavity. None of the tissues or organs of Vegf-d-deficient mice appeared swollen or distended.

Histological analysis of lymphatic vessels in the lungs of Vegf-d-deficient mice. Because the *Vegf-d* gene is highly expressed in mouse lungs during embryonic development and in adults (1, 5, 43, 47), we hypothesized that it may have a role in the development and modulation of lymphatic vessel growth in these tissues. The lungs of Vegf-d-deficient mice were compa-

TABLE 1. Body and lung masses of mice at 16 weeks of age[a]

Genotype (no. of mice in group)	Mean ± SD					
	Body mass (g)	Lung			Body mass/lung wet mass	Lung wet/dry mass
		Mass (g)		Fluid content (g)		
		Wet	Dry			
$X^+ X^+$ (6)	28.68 ± 3.88	0.19 ± 0.02	0.15 ± 0.02	0.05 ± 0.01	149.43 ± 26.83	1.31 ± 0.07
$X^- X^-$ (5)	24.59 ± 1.13	0.19 ± 0.05	0.15 ± 0.02	0.05 ± 0.03	133.97 ± 28.23	1.31 ± 0.18
X^+ Y (8)	32.36 ± 2.17	0.20 ± 0.05	0.15 ± 0.05	0.05 ± 0.02	172.85 ± 32.14	1.36 ± 0.18
X^- Y (7)	29.05 ± 3.56	0.18 ± 0.02	0.14 ± 0.02	0.05 ± 0.01	158.79 ± 21.30	1.37 ± 0.11

[a] There were no significant differences between wild-type and Vegf-d-deficient mice for any of the parameters, as assessed by the Student *t* test (in all cases, the *P* values were >0.05).

rable in mass (Table 1) and morphology to those of wild-type mice and appeared to function normally, as Vegf-d-deficient mice did not suffer difficulties with respiration. Hematoxylin and eosin staining of lung sections indicated a normal alteration of alveolar density relative to the midline in both Vegf-d-deficient and wild-type mice, reflecting bronchus and alveolar branching in the pulmonary tree (33). The alveolar densities in sections matched for position from the midline were not obviously different in Vegf-d-deficient and wild-type mice. In addition, the tissue and cellular organizations of these matched lung tissue sections, taking into consideration the apparent number and structure of bronchioles in a tissue section, were not different in Vegf-d-deficient and wild-type mice.

Immunohistochemical staining with an antibody that was raised against the extracellular domain of mouse Vegfr-3 and that detects lymphatic endothelium in normal adult tissues indicated that the lymphatic vessels of Vegf-d-deficient mouse lungs were similar in structure, appearance, and location to those of wild-type mouse lungs (Fig. 3). Typically, Vegfr-3-positive lymphatic vessels are clustered adjacent to bronchioles and the blood vessels associated with the bronchioles in the lungs (Fig. 3E and F). Counting of Vegfr-3-positive vessels immediately adjacent to the external surface of the muscular layer of bronchioles revealed a small but statistically significant reduction (as assessed by the Student *t* test) in the number of Vegfr-3-positive vessels per bronchiole in Vegf-d-deficient mice in comparison to wild-type control mice (mean ± standard deviation for Vegf-d-deficient mice, 0.80 ± 0.16 [$n = 10$]; for wild-type mice, 1.15 ± 0.14 [$n = 10$]) ($P = 0.00005$).

Analysis of lung fluid volume in Vegf-d-deficient mice. Because we observed a slight difference in the abundance of lymphatic vessels adjacent to bronchioles in the lungs of Vegf-d-deficient mice, we compared the volume of fluid within the lungs of wild-type and Vegf-d-deficient mice because this parameter can be used as an indicator of lung edema (13, 30). Lungs were excised from the chest cavity, weighed (wet mass), and dried in an oven for at least 3 days, and the mass was remeasured (dry mass). There was no significant difference in total lung masses or lung fluid compositions in wild-type and Vegf-d-deficient mice (Table 1), suggesting that Vegf-d-deficient mice have functional pulmonary lymphatic vessels.

Structure and function of large lymphatic vessels in Vegf-d-deficient mice. The mouse *Vegf-d* gene is strongly expressed immediately under the skin during embryonic development (4, 5). We therefore analyzed the function of large lymphatic vessels associated with the skin in adult Vegf-d-deficient mice. Patent Blue 5 dye, which enters lymphatic vessels but not blood vessels (14), was intradermally injected into the ventral skin of wild-type mice. The dye was specifically taken up from the interstitium into a very large lymphatic vessel that is located on the underlying surface of the ventral skin (Fig. 4A). As expected, the dye did not enter the blood vascular system during the course of this experiment, as shown by the lack of dye in the accompanying blood vessel (Fig. 4A). Furthermore, this large lymphatic vessel drained to the superficial inguinal (Fig. 4C) and axillary (Fig. 4E) lymph nodes. The locations of this lymphatic vessel, the accompanying blood vessel, and the

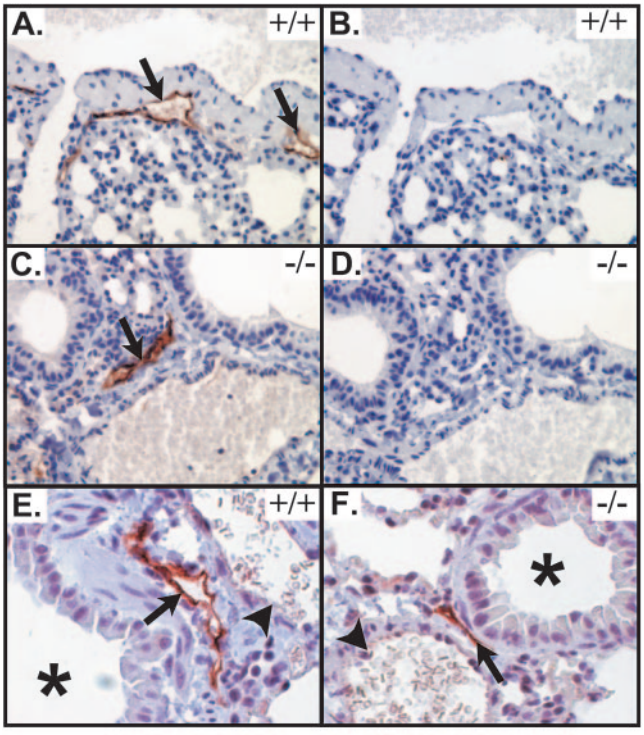

FIG. 3. Immunostaining of lungs for Vegfr-3. (A and C) Immunostaining of vessels (arrows) in the lungs of wild-type and Vegf-d-deficient mice, respectively, with Vegfr-3 monoclonal antibody. (B and D) Serial sections from panels A and C, respectively, in which the Vegfr-3 antibody was omitted from the immunostaining protocol. (E and F) Higher-power images of lung tissues obtained from wild-type and Vegf-d-deficient mice, respectively, and immunostained for Vegfr-3 show bronchioles (asterisks), Vegfr-3-positive lymphatic vessels (arrows), and blood vessels (arrowheads).

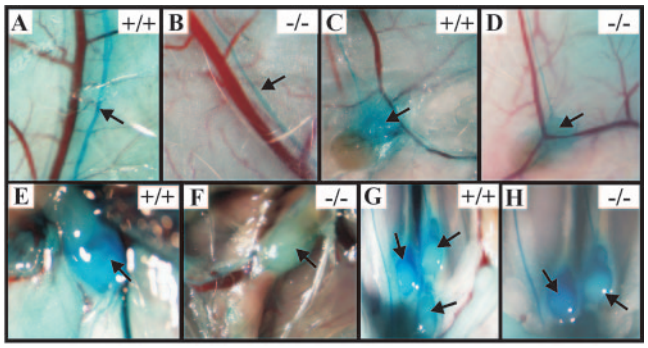

FIG. 4. Visualization of lymphatic vessels and lymph nodes by dye injection. Patent Blue 5 dye was intradermally injected into the ventral skin of wild-type (+/+) and Vegf-d-deficient (−/−) mice. The dye was taken up into a large lymphatic vessel (arrow) but not an accompanying blood vessel in the ventral skin of both wild-type (A) and Vegf-d-deficient (B) mice. The dye was transported to a superficial inguinal lymph node (arrow) of wild-type (C) and Vegf-d-deficient (D) mice as well as the draining axillary lymph node (arrow) of wild-type (E) and Vegf-d-deficient (F) mice. Uptake of the dye into the paraaortic lymph node (arrows) was also observed in wild-type (G) and Vegf-d-deficient (H) mice.

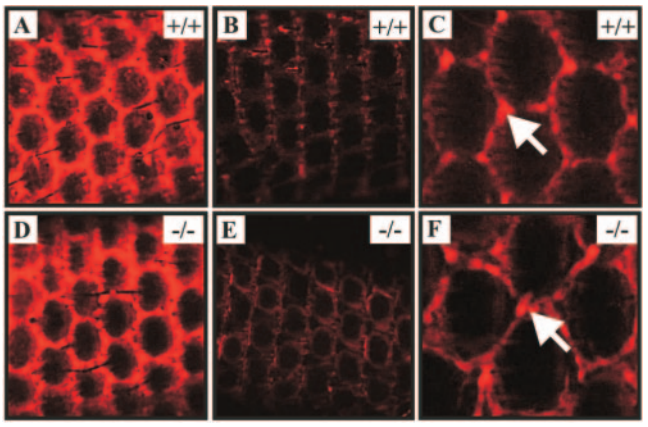

FIG. 5. Rhodamine-dextran uptake into the superficial lymphatic network of the tails of wild-type and Vegf-d-deficient mice. Rhodamine-dextran was injected into the tips of the tails of wild-type (+/+) (A) and Vegf-d-deficient (−/−) (D) mice, and uptake into the superficial lymphatic network was monitored by confocal microscopy. Uptake of the dye into lymphatic drainage ducts (arrows) of wild-type (C) and Vegf-d-deficient (F) mice was observed at higher magnifications. Autofluorescence in the tails of wild-type (B) and Vegf-d-deficient (E) mice prior to injection of the dye is also shown.

draining lymph node were similar in all of the wild-type mice studied ($n = 12$). The uptake of Patent Blue 5 dye into this large lymphatic vessel was also observed in all of the Vegf-d-deficient mice analyzed ($n = 10$) (Fig. 4B). Drainage of the dye to the superficial inguinal (Fig. 4D) and axillary (Fig. 4F) lymph nodes also occurred in the Vegf-d-deficient mice. Drainage to the paraaortic lymph nodes was also observed in wild-type and Vegf-d-deficient mice (Fig. 4G and H), suggesting that the drainage of lymph from large lymphatic vessels to lymph nodes is not significantly affected by Vegf-d deficiency.

Following injection, uptake of the dye into the large lymphatic vessel under the skin was rapid (within 5 min) in both wild-type and Vegf-d-deficient mice; no obvious difference in uptake rate was observed. Leakage of the dye from this lymphatic vessel, which would be an indicator of an abnormality of lymphatic function or endothelial cell association and/or permeability, was not observed in either wild-type or Vegf-d-deficient mice. The location of this lymphatic vessel in Vegf-d-deficient mice was also comparable to that in control mice.

Structure and function of dermal lymphatic vessels. The dermal lymphatic plexus of the mouse tail is arranged in a regular honeycomb-like pattern that allows abnormalities of lymphatic vessel density, location, and function to be readily assessed by fluorescence microlymphangiography (15, 25, 44). Rhodamine-dextran, which is specifically taken up by lymphatic vessels, was injected into the tips of mouse tails, and its distribution was monitored by fluorescence microscopy. As expected, a regular superficial lymphatic network was observed in all wild-type mice examined ($n = 20$) (Fig. 5A), and rhodamine-dextran was transported at least 3 cm along the tail from the site of injection within 15 min. No difference was observed in the pattern or rate of dye uptake into the superficial lymphatic network in Vegf-d-deficient mice ($n = 17$) (Fig. 5D). In addition, lymphatic vessel width and the maximum distance between vessels in each component of the honeycomb lymphatic pattern were not significantly different in Vegf-d-deficient mice and control mice (the P value for both parameters, as determined by the Student t test, was >0.05). At higher magnification, comparably abundant precollectors or ducts were observed in wild-type and Vegf-d-deficient mice (Fig. 5C and F). These ducts drain to deeper precollectors that, in turn, drain to deep lymphatic vessels beneath the skin (25). These findings indicate that the dermal lymphatic vasculature of Vegf-d-deficient mice is arranged in an orderly, functional configuration that is comparable to that of wild-type mice.

DISCUSSION

We hypothesized that Vegf-d may have a role in the embryonic development of the lymphatic vasculature because it is lymphangiogenic (45), it is an activating ligand for Vegfr-3 (1, 6), and it is expressed in a range of tissues during embryogenesis, when the formation of the lymphatics is taking place (5, 43). Perturbations in lymphatic development or function may be manifested as tissue edema and accumulation of chyle in the intestines or peritoneal cavity, as was observed in mutant mice deficient in Vegf-c (20), the homeobox protein Prox1 (46), or angiopoietin 2, a ligand for endothelial cell receptor Tie2 (12). Therefore, it was surprising that there was no evidence of edema in the skin or organs of Vegf-d-deficient mice, nor was there an abnormal accumulation of chyle in the intestines or peritoneal cavity. The lymphatic vessels and lymph nodes appeared to develop and function normally, as indicated by immunohistochemical and microlymphangiographic studies. Furthermore, the lymphatics of Vegf-d-deficient mice were similar in width, location, and structural integrity to those of wild-type mice and were capable of transporting fluid to lymph nodes in the axillary and inguinal regions and to deep lymph nodes surrounding the descending aorta. Therefore, inactivation of the *Vegf-d* gene alone does not significantly perturb lymphatic development and clearly does not phenocopy the overt phenotype exhibited by Vegfr-3-deficient mice, which die during

early embryonic development from defects in the remodeling of large blood vessels, before the lymphatic vessels emerge (11).

The lack of a profound lymphatic vessel defect in Vegf-d-deficient mice may reflect a subtle, redundant, or nonexistent role for this growth factor during embryonic development. Nonetheless, Vegf-d may induce lymphatic vessel growth in adult life in response to pathological conditions. Vegf-d-deficient mice represent an opportunity to study such putative roles by analyzing the effects of physiological or pathological challenges. This study also suggests that there may be functional redundancy within the VEGF family. The most likely candidate for compensating for Vegf-d deficiency is Vegf-c. Vegf-c is highly homologous to Vegf-d (1, 17), is the only other known activator of Vegfr-3 (17), has an expression pattern partly overlapping that of Vegf-d (1, 4, 5, 43, 23, 24), and is critical for the development of the lymphatic vasculature (20). We did not, however, find any evidence of Vegf-c up-regulation in the tissues of Vegf-d-deficient mice by Northern blotting, suggesting that if such compensation occurs, then it does so without a requirement for significantly enhanced levels of Vegf-c mRNA.

Inactivation of the *Vegfr-3* gene in mice causes death at E9.5 in association with defective remodeling of blood vessels (11), whereas inactivation of the mouse *Vegf-c* gene leads to death of embryos between E15.5 and birth due to fluid accumulation in tissues as a consequence of a lack of lymphatic vessels (20). As Vegf-c and Vegf-d are the only known ligands for Vegfr-3, we anticipated that Vegf-d function might account for the difference between the phenotypes of *Vegf-c*$^{-/-}$ and *Vegfr-3*$^{-/-}$ mice. The lack of a profound phenotype in Vegf-d-deficient mice raises the possibility that Vegf-d may not function in Vegf-c-deficient mice to allow them to survive longer than Vegfr-3-deficient mice but rather that other, as-yet-unknown signaling mechanisms via Vegfr-3 could be involved during the early development of blood vessels. Such mechanisms could involve other soluble Vegfr-3 ligands or cell surface-ssociated molecules. The generation of mice doubly deficient for Vegf-c and Vegf-d will be required to explore this issue more conclusively.

The findings presented here indicate that Vegf-c-mediated signaling is more important for the development of the lymphatic vasculature during embryogenesis than is signaling induced by Vegf-d. It is noteworthy that a range of in vivo delivery approaches have demonstrated that Vegf-d can induce lymphangiogenesis and angiogenesis in normal tissues and pathological conditions, such as cancer (10, 36, 37, 42, 45). Therefore, the biological functions of Vegf-d may be revealed in the response to disease or tissue damage rather than in the context of embryonic development.

ACKNOWLEDGMENTS

This work was supported by grants from the National Health and Medical Research Council of Australia (NH&MRC) and the Cancer Council of Victoria, Australia (CCV). M.E.B. was supported by a postdoctoral fellowship from the CCV, S.A.S. was supported by a Pfizer Foundation senior research fellowship, and M.G.A. and M.L.H. were supported by senior research fellowships from the NH&MRC.

We thank Shin-Ichi Nishikawa for antibody against Vegfr-3, Patricia Lai, Dimitria Vranes, and Gillian Thornton for technical assistance, Peter Lock for DokR antiserum, and Tony Burgess for constructive comments.

REFERENCES

1. **Achen, M. G., M. Jeltsch, E. Kukk, T. Mäkinen, A. Vitali, A. F. Wilks, K. Alitalo, and S. A. Stacker.** 1998. Vascular endothelial growth factor D (VEGF-D) is a ligand for the tyrosine kinases VEGF receptor 2 (Flk-1) and VEGF receptor 3 (Flt-4). Proc. Natl. Acad. Sci. USA **95:**548–553.
2. **Achen, M. G., S. Roufail, T. Domagala, B. Catimel, E. C. Nice, D. M. Geleick, R. Murphy, A. M. Scott, C. Caesar, T. Makinen, K. Alitalo, and S. A. Stacker.** 2000. Monoclonal antibodies to vascular endothelial growth factor-D block interactions with both VEGF receptor-2 and VEGF receptor-3. Eur. J. Biochem. **267:**2505–2515.
3. **Achen, M. G., R. A. Williams, M. E. Baldwin, P. Lai, S. Roufail, K. Alitalo, and S. A. Stacker.** 2002. The angiogenic and lymphangiogenic factor vascular endothelial growth factor-D exhibits a paracrine mode of action in cancer. Growth Factors **20:**99–107.
4. **Achen, M. G., R. A. Williams, M. P. Minekus, G. E. Thornton, K. Stenvers, P. A. W. Rogers, F. Lederman, S. Roufail, and S. A. Stacker.** 2001. Localization of vascular endothelial growth factor-D in malignant melanoma suggests a role in tumour angiogenesis. J. Pathol. **193:**147–154.
5. **Avantaggiato, V., M. Orlandini, D. Acampora, S. Oliviero, and A. Simeone.** 1998. Embryonic expression pattern of the murine *figf* gene, a growth factor belonging to platelet-derived growth factor/vascular endothelial growth factor family. Mech. Dev. **73:**221–224.
6. **Baldwin, M. E., B. Catimel, E. C. Nice, S. Roufail, N. E. Hall, K. L. Stenvers, M. J. Karkkainen, K. Alitalo, S. A. Stacker, and M. G. Achen.** 2001. The specificity of receptor binding by vascular endothelial growth factor-D is different in mouse and man. J. Biol. Chem. **276:**19166–19171.
7. **Baldwin, M. E., S. Roufail, M. M. Halford, K. Alitalo, S. A. Stacker, and M. G. Achen.** 2001. Multiple forms of mouse vascular endothelial growth factor-D are generated by RNA splicing and proteolysis. J. Biol. Chem. **276:**44307–44314.
8. **Baldwin, M. E., S. A. Stacker, and M. G. Achen.** 2002. Molecular control of lymphangiogenesis. Bioessays **24:**1030–1040.
9. **Barnett, L. D., and F. Kontgen.** 2001. Gene targeting in a centralized facility. Methods Mol. Biol. **158:**65–82.
10. **Bhardwaj, S., H. Roy, M. Gruchala, H. Viita, I. Kholova, I. Kokina, M. G. Achen, S. A. Stacker, M. Hedman, K. Alitalo, and S. Yla-Herttuala.** 2003. Angiogenic responses of vascular endothelial growth factors in periadventitial tissue. Hum. Gene Ther. **14:**1451–1562.
11. **Dumont, D. J., L. Jussila, J. Taipale, A. Lymboussaki, T. Mustonen, K. Pajusola, M. Breitman, and K. Alitalo.** 1998. Cardiovascular failure in mouse embryos deficient in VEGF receptor-3. Science **282:**946–949.
12. **Gale, N. W., G. Thurston, S. F. Hackett, R. Renard, Q. Wang, J. McClain, C. Martin, C. Witte, M. H. Witte, D. Jackson, C. Suri, P. A. Campochiaro, S. J. Wiegand, and G. D. Yancopoulos.** 2002. Angiopoietin-2 is required for postnatal angiogenesis and lymphatic patterning, and only the latter role is rescued by angiopoietin-1. Dev. Cell **3:**411–423.
13. **Guery, B. P., S. Nelson, N. Viget, P. Fialdes, W. R. Summer, E. Dobard, G. Beaucaire, and C. M. Mason.** 1998. Fluorescein-labeled dextran concentration is increased in BAL fluid after ANTU-induced edema in rats. J. Appl. Physiol. **85:**842–848.
14. **Jansen, L., M. H. Doting, E. J. Rutgers, J. de Vries, R. A. Olmos, and O. E. Nieweg.** 2000. Clinical relevance of sentinel lymph nodes outside the axilla in patients with breast cancer. Br. J. Surg. **87:**920–925.
15. **Jeltsch, M., A. Kaipainen, V. Joukov, X. Meng, M. Lakso, H. Rauvala, M. Swartz, D. Fukumura, R. K. Jain, and K. Alitalo.** 1997. Hyperplasia of lymphatic vessels in VEGF-C transgenic mice. Science **276:**1423–1425.
16. **Jenkins, N. A., E. Woollatt, J. Crawford, D. J. Gilbert, M. E. Baldwin, G. R. Sutherland, N. G. Copeland, and M. G. Achen.** 1997. Mapping of the gene for vascular endothelial growth factor-D in mouse and man to the X chromosome. Chromosome Res. **5:**502–505.
17. **Joukov, V., K. Pajusola, A. Kaipainen, D. Chilov, I. Lahtinen, E. Kukk, O. Saksela, N. Kalkkinen, and K. Alitalo.** 1996. A novel vascular endothelial growth factor, VEGF-C, is a ligand for the Flt-4 (VEGFR-3) and KDR (VEGFR-2) receptor tyrosine kinases. EMBO J. **15:**290–298.
18. **Kaipainen, A., J. Korhonen, T. Mustonen, V. W. van Hinsbergh, G. H. Fang, D. Dumont, M. Breitman, and K. Alitalo.** 1995. Expression of the fms-like tyrosine kinase 4 gene becomes restricted to lymphatic endothelium during development. Proc. Natl. Acad. Sci. USA **92:**3566–3570.
19. **Karkkainen, M. J., R. E. Ferrell, E. C. Lawrence, M. A. Kimak, K. L. Levinson, M. A. McTigue, K. Alitalo, and D. N. Finegold.** 2000. Missense mutations interfere with VEGFR-3 signalling in primary lymphoedema. Nat. Genet. **25:**153–159.
20. **Karkkainen, M. J., P. Haiko, K. Sainio, J. Partanen, J. Taipale, T. V. Petrova, M. Jeltsch, D. G. Jackson, M. Talikka, H. Rauvala, C. Betsholtz, and K. Alitalo.** 2004. Vascular endothelial growth factor C is required for sprouting of the first lymphatic vessels from embryonic veins. Nat. Immunol. **5:**74–80.
21. **Karpanen, T., M. Egeblad, M. J. Karkkainen, H. Kubo, S. Ylä-Herttuala, M. Jäättelä, and K. Alitalo.** 2001. Vascular endothelial growth factor C pro-

motes tumor lymphangiogenesis and intralymphatic tumor growth. Cancer Res. **61:**1786–1790.
22. **Kubo, H., T. Fujiwara, L. Jussila, H. Hashi, M. Ogawa, K. Shimizu, M. Awane, Y. Sakai, A. Takabayashi, K. Alitalo, Y. Yamaoka, and S.-I. Nishikawa.** 2000. Involvement of vascular endothelial growth factor receptor-3 in maintenance of integrity of endothelial cell lining during tumor angiogenesis. Blood **96:**546–553.
23. **Kukk, E., A. Lymboussaki, S. Taira, A. Kaipainen, M. Jeltsch, V. Joukov, and K. Alitalo.** 1996. VEGF-C receptor binding and pattern of expression with VEGFR-3 suggests a role in lymphatic vascular development. Development **122:**3829–3837.
24. **Lee, J., A. Gray, J. Yuan, S. M. Luoh, H. Avraham, and W. I. Wood.** 1996. Vascular endothelial growth factor-related protein: a ligand and specific activator of the tyrosine kinase receptor Flt4. Proc. Natl. Acad. Sci. USA **93:**1988–1992.
25. **Leu, A. J., D. A. Berk, F. Yuan, and R. K. Jain.** 1994. Flow velocity in the superficial lymphatic network of the mouse tail. Am. J. Physiol. **267:**H1507–H1513.
26. **Lock, P., F. Casagranda, and A. R. Dunn.** 1999. Independent SH2-binding sites mediate interaction of Dok-related protein with RasGTPase-activating protein and Nck. J. Biol. Chem. **274:**22775–22784.
27. **Lymboussaki, A., T. A. Partanen, B. Olofsson, J. Thomas-Crusells, C. D. M. Fletcher, R. M. W. de Waal, A. Kaipainen, and K. Alitalo.** 1998. Expression of the vascular endothelial growth factor C receptor VEGFR-3 in lymphatic endothelium of the skin and in vascular tumors. Am. J. Pathol. **153:**395–403.
28. **Mäkinen, T., L. Jussila, T. Veikkola, T. Karpanen, M. I. Kettunen, K. J. Pulkkanen, R. Kauppinen, D. G. Jackson, H. Kubo, S. I. Nishikawa, S. Ylä-Herttuala, and K. Alitalo.** 2001. Inhibition of lymphangiogenesis with resulting lymphedema in transgenic mice expressing soluble VEGF receptor-3. Nat. Med. **7:**199–205.
29. **Mandriota, S. J., L. Jussila, M. Jeltsch, A. Compagni, D. Baetens, R. Prevo, S. Banerji, J. Huarte, R. Montesano, D. G. Jackson, L. Orci, K. Alitalo, G. Christofori, and M. S. Pepper.** 2001. Vascular endothelial growth factor-C-mediated lymphangiogenesis promotes tumour metastasis. EMBO J. **20:**672–682.
30. **Mason, C. M., B. P. Guery, W. R. Summer, and S. Nelson.** 1996. Keratinocyte growth factor attenuates lung leak induced by alpha-naphthylthiourea in rats. Crit. Care Med. **24:**925–931.
31. **McColl, B. K., M. E. Baldwin, S. Roufail, C. Freeman, R. L. Moritz, R. J. Simpson, K. Alitalo, S. A. Stacker, and M. G. Achen.** 2003. Plasmin activates the lymphangiogenic growth factors VEGF-C and VEGF-D. J. Exp. Med. **198:**863–868.
32. **Millauer, B., S. Wizigmann-Voos, H. Schnürch, R. Martinez, N. P. H. Moller, W. Risau, and A. Ullrich.** 1993. High affinity VEGF binding and developmental expression suggest Flk-1 as a major regulator of vasculogenesis and angiogenesis. Cell **72:**835–846.
33. **Moore, K. L.** 1985. Clinically orientated anatomy. The Williams & Wilkins Co., Baltimore, Md.
34. **Nagy, J. A., E. Vasile, D. Feng, C. Sundberg, L. F. Brown, M. J. Detmar, J. A. Lawitts, L. Benjamin, X. Tan, E. J. Manseau, A. M. Dvorak, and H. F. Dvorak.** 2002. Vascular permeability factor/vascular endothelial growth factor induces lymphangiogenesis as well as angiogenesis. J. Exp. Med. **196:**1497–1506.
35. **Orlandini, M., L. Marconcini, R. Ferruzzi, and S. Oliviero.** 1996. Identification of a c-*fos*-induced gene that is related to the platelet-derived growth factor/vascular endothelial growth factor family. Proc. Natl. Acad. Sci. USA **93:**11675–11680.
36. **Rissanen, T. T., J. E. Markkanen, M. Gruchala, T. Heikura, A. Puranen, M. I. Kettunen, I. Kholová, R. A. Kauppinen, M. G. Achen, S. A. Stacker, K. Alitalo, and S. Ylä-Herttuala.** 2003. VEGF-D is the strongest angiogenic and lymphangiogenic effector among VEGFs delivered into skeletal muscle via adenoviruses. Circ. Res. **92:**1098–1106.
37. **Rutanen, J., T. T. Rissanen, J. E. Markkanen, M. Gruchala, P. Silvennoinen, A. Kivela, A. Hedman, M. Hedman, T. Heikura, M. R. Orden, S. A. Stacker, M. G. Achen, J. Hartikainen, and S. Yla-Herttuala.** 2004. Adenoviral catheter-mediated intramyocardial gene transfer using the mature form of vascular endothelial growth factor-D induces transmural angiogenesis in porcine heart. Circulation **109:**1029–1035.
38. **Sambrook, J., and D. W. Russell.** 2001. Molecular cloning: a laboratory manual, 3nd ed. Cold Spring Harbor Laboratory Press, Cold Spring Harbor, N.Y.
39. **Skobe, M., T. Hawighorst, D. G. Jackson, R. Prevo, L. Janes, P. Velasco, L. Riccardi, K. Alitalo, K. Claffey, and M. Detmar.** 2001. Induction of tumor lymphangiogenesis by VEGF-C promotes breast cancer metastasis. Nat. Med. **7:**192–198.
40. **Stacker, S. A., M. G. Achen, L. Jussila, M. E. Baldwin, and K. Alitalo.** 2002. Lymphangiogenesis and cancer metastasis. Nat. Rev. Cancer **2:**573–583.
41. **Stacker, S. A., M. E. Baldwin, and M. G. Achen.** 2002. The role of tumor lymphangiogenesis in metastatic spread. FASEB J. **16:**922–934.
42. **Stacker, S. A., C. Caesar, M. E. Baldwin, G. E. Thornton, R. A. Williams, R. Prevo, D. G. Jackson, S.-I. Nishikawa, H. Kubo, and M. G. Achen.** 2001. VEGF-D promotes the metastatic spread of tumor cells via the lymphatics. Nat. Med. **7:**186–191.
43. **Stacker, S. A., K. Stenvers, C. Caesar, A. Vitali, T. Domagala, E. Nice, S. Roufail, R. J. Simpson, R. Moritz, T. Karpanen, K. Alitalo, and M. G. Achen.** 1999. Biosynthesis of vascular endothelial growth factor-D involves proteolytic processing which generates non-covalent homodimers. J. Biol. Chem. **274:**32127–32136.
44. **Swartz, M. A., D. A. Berk, and R. K. Jain.** 1996. Transport in lymphatic capillaries. I. Macroscopic measurements using residence time distribution theory. Am. J. Physiol. **270:**H324–H329.
45. **Veikkola, T., L. Jussila, T. Makinen, T. Karpanen, M. Jeltsch, T. V. Petrova, H. Kubo, G. Thurston, D. M. McDonald, M. G. Achen, S. A. Stacker, and K. Alitalo.** 2001. Signalling via vascular endothelial growth factor receptor-3 is sufficient for lymphangiogenesis in transgenic mice. EMBO J. **20:**1223–1231.
46. **Wigle, J. T., and G. Oliver.** 1999. *Prox1* function is required for the development of the murine lymphatic system. Cell **98:**769–778.
47. **Yamada, Y., J.-I. Nezu, M. Shimane, and Y. Hirata.** 1997. Molecular cloning of a novel vascular endothelial growth factor, VEGF-D. Genomics **42:**483–488.